RSC Advances

PAPER

View Article Online
View Journal | View Issue

Check for updates

Cite this: *RSC Adv.*, 2024, **14**, 25093

Ag/Cu doped polyaniline hybrid nanocomposite-based novel gas sensor for enhanced ammonia gas sensing performance at room temperature

Arunima Verma and Tanuj Kumar *

Hybrid nanocomposites, which comprise organic and inorganic materials, have gained increasing attention in applications for enhanced sensing response to both reducing and oxidation gases. In this study, a novel nanocomposite is synthesized using chemical polymerization by reinforcing Ag/Cu nanoparticles with different concentrations doped into the polyaniline matrix. This hybrid nanocomposite is used as a sensing platform for ammonia detection with different concentrations (ppm). The homogeneous distribution of Ag/Cu nanoparticles onto the PANI matrix provides a smooth and dense surface area, further accelerating the transmission of electrons. The synergistic effect of the PANI@Ag/Cu matrix is responsible for the outstanding conductivity, compatibility, and catalytic ability of the proposed gas sensor. The structure, morphology, and surface composition of as-synthesized samples were examined using X-ray diffraction, field emission scanning electron microscopy, ultraviolet-visible spectroscopy, energy dispersive spectroscopy, thermogravimetric analysis, and Fourier transform infrared spectroscopy. The results indicated that the resistive sensor based on the PANI@Ag/Cu_3 hybrid nanocomposite exhibited the highest response toward ammonia at room temperature, with a response value of 86% to a concentration of 300 ppm. We also investigated the sensing properties of volatile organic compounds, including carbon dioxide, carbon monoxide, ethanol and hydrogen sulphide. Characterization and gas sensing measurements exhibited protonation and deprotonation of the PANI@Ag/Cu heterojunction, which contributes to the ammonia sensing mechanism. Overall, the obtained findings demonstrated that the PANI@Ag/Cu hybrid nanocomposite is a promising material for gas sensing applications in environmental monitoring.

Received 31st May 2024
Accepted 29th July 2024

DOI: 10.1039/d4ra04009k

rsc.li/rsc-advances

Open Access Article. Published on 12 2024. Downloaded on 06.08.2025 02:01:24.
This article is licensed under a Creative Commons Attribution-NonCommercial 3.0 Unported Licence.

1. Introduction

Environmental degradation has been greatly exacerbated by the rapid advancement of civilization. Environmental and pollution management are becoming increasingly important as enterprises grow. We must study more about harmful gases such as CO, NO_2, NH_3, CO_2 and other hydrocarbons to protect humans and ecosystems. Usually, gas sensors detect gas concentrations.[1,2] The past few decades have seen the development of many gas sensors with different detecting materials and signal transmission mechanisms. Conducting polymer composites, metal oxide/polymer composites, and metal oxide semiconductors are useful sensing materials. Due to their remarkable mechanical properties, conducting polymer composites have garnered the attention of researchers.[3] Compared to other intrinsically conducting polymers, polyaniline (PANI) has several advantages, such as ease of synthesis, cheap monomer, tunable characteristics, high conductivity, and high stability. Graphene oxide (GO), reduced graphene oxide (rGO), and carbon nanotubes (CNTs) are some of the more common carbon-based matrices used in gas sensors; nevertheless, PANI is superior to them in every aspect. In addition to its intrinsic electrical conductivity, PANI can be easily doped and de-doped to customise sensor responses and this trait helps detect several gases sensitively. As an environmentally stable and chemically resistant material, PANI gas sensors survive longer and operate better. PANI nanofibers, nanotubes, and nanospheres boost sensor performance by providing a large gas adsorption surface area. PANI can be functionalized with different dopants and composites to make selective gas sensors because it is easier to synthesise and deposit than GO and RGO. Although CNTs offer outstanding electrical properties, manufacturing and functionalizing CNT-based sensors is laborious and expensive. PANI can be used to make sensitive, stable, and efficient gas sensors at a lower cost. The conducting polymer can be doped chemically, electrochemically, or photochemically to change its conductivity.[4] If ions are able to migrate from a dopant to a polymer or *vice versa*, then conductivity can be defined as the ability of their movement.[5] The ways in which PANI and noble metals interact with one another are of interest to a wide variety of fields and specialties. Metal–PANI composites have a wide

Department of Nanoscience & Materials, Central University of Jammu, Jammu, 181143, India. E-mail: tanuj.nsm@cujammu.ac.in

© 2024 The Author(s). Published by the Royal Society of Chemistry

Open Access Article. Published on 12 2024. Downloaded on 06.08.2025 02:01:24.
This article is licensed under a Creative Commons Attribution-NonCommercial 3.0 Unported Licence.

range of applications, including but not limited to the following: gas sensors,[6,7] biosensors,[8,9] electrochemical sensors[10] and supercapacitors.[11] Interestingly, inorganic sensitive materials have different gas sensor benefits than conducting polymers. For example, metal oxides are highly sensitive because of their oxygen stoichiometry and active surface charge,[12] but they can only be used at very high temperatures, which limits their practicality. To improve gas sensor performance, metal nanostructures are used as sensitivity enhancers due to chemical and electronic sensitization effects.[13] There is a lot of interest in gas-sensing applications because conducting polymer–inorganic nanocomposite may produce high-performance gas sensors owing to their synergistic effects. Enhanced or new chemical and physical functions may be provided by the weak van der Waals, hydrogen, covalent, or ionic covalent bonding, interacting with the host organic and guest inorganic phases in the nanocomposite system. Due to their synergistic and complementary effects, nanocomposite materials and gas sensors could overcome their weaknesses while maximising the strengths of their respective components in gas-sensing applications. Metal nanostructures based on Pd,[14] Au,[15] Ag,[16] Cu[17] and other elements have been extensively explored for their potential use in gas sensing due to their strong electrocatalytic activity and also superior stability. Gas sensors may benefit greatly from employing nanostructured metals based on Ag and Cu, two of the most extensively used profitable catalysts at low cost. Doping the polymer with metal NPs may drastically alter its electrical characteristics, and the resulting system shows remarkable ability to adsorb and desorb reducing gases at room temperature (H_2, CO, NH_3). It has been demonstrated that the type, quantity and size of metal nanophase utilized in composites significantly affect the electrical conductivity of a material. Nanostructured metals were combined with conducting polymers using a wide variety of methods, including hydrothermal synthesis,[18] *in situ* chemical oxidative polymerizing,[16] self-assembling,[15,19] template based vapour deposition polymerization (VDP), and *in situ* photopolymerization. For instance, several such works are underway for gas sensing: Shivam Kumar *et al.*[20] created a highly sensitive Cu ethylenediamine/PANI composite film to measure formaldehyde; Zhang *et al.*[21] created a PANI/Ag nanocomposite and S. Cuiab *et al.*[22] used layer-by-layer self-assembly to create a PANI/TiO_2 nanocomposite film. Nanocomposites performed linearly with metal concentration, but much remains to be learned about their performance compared to pure PANI.

Research into ternary hybrid systems has been growing in popularity as a means to improve sensing performance. Metal particle–metal oxide–conducting polymers, metal particle–carbon nanotubes–conducting polymers, metal particle–graphene–conducting polymers, metal oxide–graphene conducting polymers and metal oxide–metal oxide–conducting polymers[23,24] are among the gas sensors based on ternary nanocomposite that have been synthesised for gas-sensing research. The carboxylated polypyrrole (CPPy)/CNTs/Pd nanocomposites produced by Park *et al.*[23] for NH_3 detection are simple and novel. By *in situ* polymerization, Zhang *et al.*[25] synthesised ZnO, graphene quantum dots (GQDs), and PANI nanocomposites. At room temperature, ZnO, GQDs, and PANI nanocomposite sensors showed high sensitivity (from 2% to 500 ppb acetone), selectivity, response/recovery time of 15/27 s, reproducibility, and long-term stability. Additionally, the conductive polymer-based ternary material mixture system is not random. Process compatibility, morphology, composition ratio and function distribution are the only ways to achieve synergistic reinforcement of many materials. Utilising Ag/Cu and PANI characteristics, this research aims to create a unique ammonia detection device. Reasons to assume Ag/Cu can improve conducting polymer sensing include the following: polymer conductivity is altered by Ag/Cu nanoparticles. Secondly, Ag/Cu nanoparticles may improve sensor selectivity as chemical receptors and various metal nanoparticles exhibit chemical affinity for gas molecules. Metal-containing conductive polymers improve nanocomposite–gas interaction. These aspects inspired the development of a hybrid conducting polymer nanocomposite ammonia gas sensor based on *in situ* Ag/Cu synthesis in a PANI matrix for room-temperature performance. PANI@Ag/Cu hybrid nanocomposite can be prepared with a range of five different concentrations of silver nitrate and copper acetate. Analysis of the conducting polymer and its nanocomposites was carried out using XRD, UV, FESEM, EDS, TGA and FT-IR methods. To create PANI and PANI@Ag/Cu hybrid nanocomposite films, the spin-coating technique was applied to a silicon substrate. The gas-sensing capabilities of the samples were examined by subjecting them to different concentrations of NH_3 at room temperature. In addition, the mechanisms and impacts of Ag/Cu on sensor behaviour for ammonia detection were thoroughly examined. Among the many practical benefits of environmental monitoring, the study emphasizes the fact that the PANI@Ag/Cu hybrid nanocomposite can achieve its increased sensing capabilities at room temperature. To the best of our knowledge, no research has been carried out thus far on gas sensors based on PANI@Ag/Cu hybrid nanocomposite films, which could improve the room temperature detection performance of ammonia gas.

2. Experimental procedure

2.1 Materials required

Ammonium persulfate (APS) (M.W. 228.20 g mol^{-1}, Sigma-Aldrich), silver nitrate ($AgNO_3$ g mol^{-1}) (M.W. 169.87, Sigma-Aldrich), copper acetate $Cu(OAc_2)$ (M.W. 181.63 g mol^{-1}, Sigma-Aldrich), aniline monomer (M.W. 93.13, AR), and hydrochloric acid (M.W. 36.46 g mol^{-1}. AR) were procured. No additional purification was performed on the other reagents prior to use. All solutions used in the experiment were prepared using double distilled water.

2.2 Synthesis of polyaniline (PANI)

PANI was synthesized using a method involving the mixing of solutions. Scheme 1 shows the use of ammonium persulfate as an oxidant/initiator in conjunction with aniline polymerization in concentrated hydrochloric acid to produce an acidic medium. Aniline (0.925 mL) in distilled water (10 mL) and HCl

© 2024 The Author(s). Published by the Royal Society of Chemistry

Open Access Article. Published on 12 2024. Downloaded on 06.08.2025 02:01:24.
This article is licensed under a Creative Commons Attribution-NonCommercial 3.0 Unported Licence.

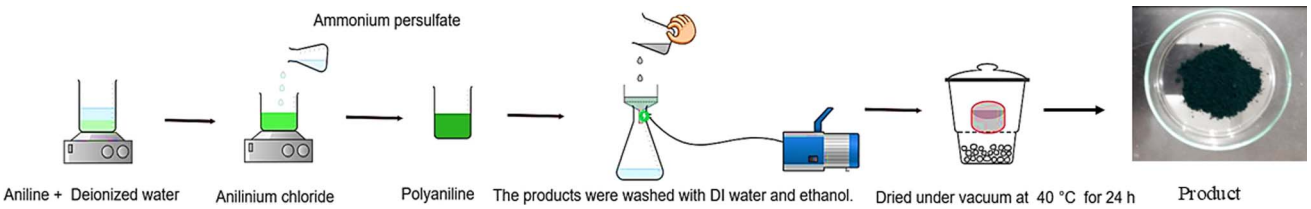

Scheme 1 Aniline and ammonium persulfate are used in the synthesis of PANI in an acidic medium.

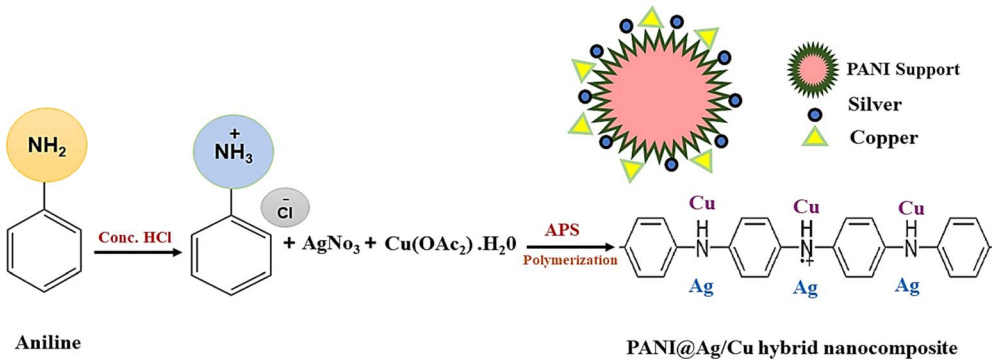

Scheme 2 Methods for the preparation of PANI @Ag/Cu hybrid nanocomposite.

(0.25 mL) were prepared in a beaker according to a typical procedure. This process results in the pH of the solution being approximately 6.16. After being stirred, the reaction mixture was cooled to a temperature between 0–5 °C for approximately fifteen minutes. Subsequently, a solution of ammonium persulfate (0.5 g in 10 mL distilled water) was gradually added dropwise to the aforementioned reaction mixture while being continuously stirred; this process took exactly 2 hours to complete. The pH of the solution after adding ammonium persulfate solution is approximately 4.97. The reaction mixture was stirred for three hours until a solid precipitate formed, and then it was left overnight to set. The large molecular weight of the polymer (PANI) causes it to drop to the bottom, while the unreacted aniline and oligomer stay suspended in the supernatant and are separated by decantation. 10 mL of distilled water was incorporated upon decantation and let sit for 2 hours. The process was performed twice to remove any aniline or oligomers, with the supernatant eliminated after repetition. Then, distilled water and ethanol were used to wash the precipitate after it had been obtained by filtering. The sample was obtained by drying in an oven set at 40 °C.[26]

2.3 Synthesis of PANI@Ag/Cu hybrid nanocomposite

In this study, the hybrid nanocomposite of polyaniline (PANI) and metal was prepared using the oxidative polymerization method, as shown in Scheme 2. Prepare a solution containing 0.92 mL aniline monomer dissolved in a 0.25 mL hydrochloric acidic solution. Dissolve separate amounts of 0.2 g silver nitrate ($AgNO_3$) and copper acetate $Cu(OAc_2)$ in distilled water to obtain metal salt solutions. Mix the aniline solution with the individual metal salt solutions in specific proportions to achieve the desired composition. Stir the mixture thoroughly to ensure homogeneity. Add 0.1 g of oxidizing agent such as ammonium persulfate (APS) to the mixture containing aniline and metal salt solutions. The oxidation process will initiate the polymerization of aniline into PANI and simultaneously lead to the reduction of metal ions, forming Ag and Cu nanoparticles within the PANI matrix. The mixture was stirred until the solution changed to a greenish-dark brown liquid, indicating the formation of PANI@Ag/Cu hybrid nanocomposite. Filter the nanocomposite solution to collect the solid material using a filtration apparatus. Wash the collected composite thoroughly with distilled water and ethanol to remove any residual chemicals. Dry the PANI@Ag/Cu nanocomposite in an oven at a controlled temperature to remove any remaining solvent. Various concentrations of Ag were combined with PANI films.[27] PANI@Ag/Cu hybrid nanocomposites were prepared with different concentrations of silver nitrate and copper acetate (0.15, 0.3, 0.6, 0.9 and 1.2 M), hereafter called PANI@Ag/Cu_1, PANI@Ag/Cu_2, PANI@Ag/Cu_3, PANI@Ag/Cu_4 and PANI@Ag/Cu_5, respectively, as shown in Table 1.

Table 1 PANI with various concentrations of silver nitrate and copper acetate

Sample	PANI (ML)	Silver nitrate (G)	Copper acetate (G)
Pure pani	10	0	0
Pani@Ag/Cu_1	10	0.2	2.0
Pani@Ag/Cu_2	10	0.5	0.5
Pani@Ag/Cu_3	10	1	1
Pani@Ag/Cu_4	10	1.5	1.5
Pani@Ag/Cu_5	10	2	2

Open Access Article. Published on 12 2024. Downloaded on 06.08.2025 02:01:24.
This article is licensed under a Creative Commons Attribution-NonCommercial 3.0 Unported Licence.

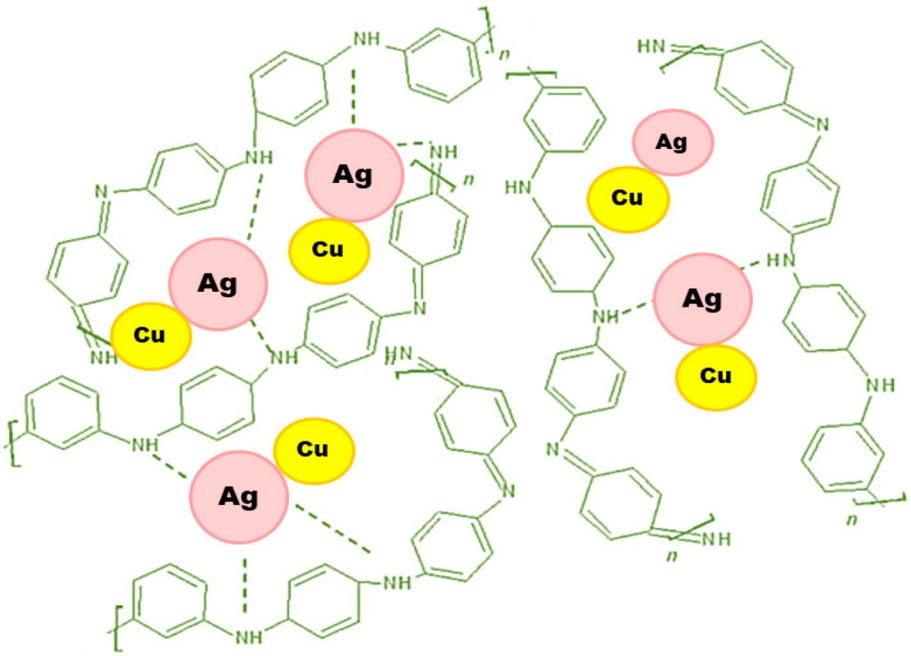

Scheme 3 Stabilization mechanism of PANI@Ag/Cu hybrid nanocomposite.

Nitrogen atoms in PANI amine and imine groups can coordinate with metal ions. A coordination link can be formed between these nitrogen atoms and either silver or copper, stabilising the metal nanoparticles within the PANI matrix. Synthesis of the hybrid nanocomposite can involve redox reactions in which PANI can reduce Ag^{+} and Cu^{2+} ions to their corresponding metallic forms, Cu^{0} and Ag^{0}, respectively. As a consequence of this procedure, metal nanoparticles are created without external sources within the PANI matrix. The inclusion of Ag and Cu nanoparticles into the PANI matrix can improve its electrical conductivity because these metals are very conductive. All things considered, the nanocomposite performance in gas sensing and similar applications is enhanced by this synergistic effect. As shown in Scheme 3, the amine groups included in PANI inhibit the aggregation of Ag/Cu nanoparticles.[28]

3. Results and discussion

3.1 X-ray diffraction

The X-ray diffraction patterns of PANI@Ag/Cu hybrid nanocomposite are shown in Fig. 1. The diffraction patterns of PANI reveal the presence of both crystalline and amorphous components as evidenced by the peaks at 2θ of approximately 11.66°, 18.38°, 20.43° and 25.55°. Similar to the findings of Bhagwat *et al.*,[29] the crystalline PANI is attributed to the planar nature of the benzenoid and quinoid functional groups and the nanofiber structure. The parallel periodicity of the polymer chain corresponds to the peak at approximately 20.43°, while the monoclinic periodicity may be linked to the peak at approximately 26.36°. For the XRD pattern of the PANI@Ag/Cu hybrid nanocomposite, besides the PANI broad peak, the narrow peaks indicate the high degree of crystallinity of Ag and Cu in a face-

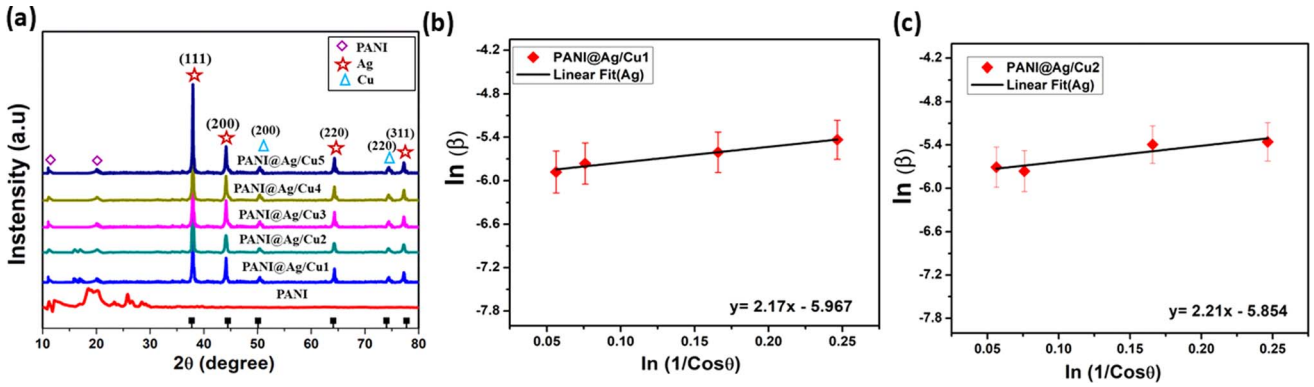

Fig. 1 The XRD spectra of (a) PANI and PANI@Ag/Cu hybrid nanocomposite with the concentration ratios of Ag/Cu and (b and c) Williamson–Hall plot of nano-crystallite silver sample.

© 2024 The Author(s). Published by the Royal Society of Chemistry

Open Access Article. Published on 12 2024. Downloaded on 06.08.2025 02:01:24.
This article is licensed under a Creative Commons Attribution-NonCommercial 3.0 Unported Licence.

Table 2 The calculated crystallite size of PANI@Ag/Cu hybrid nanocomposite

Conc. (g)	2θ of the intense peak (degree) Ag	Cu	FWHM of intense peak (β) radians Ag	Cu	Crystallite size (nm) Ag	Cu	d-Spacing nm Ag	Cu	Lattice parameter (a) Å Ag	Cu	Macrostrain ($\varepsilon \times 10^{-3}$) Ag	Cu	Dislocation density ($\delta \times 10^{-3}$ nm^{-2}) Ag	Cu
0.2	38.16	50.41	0.0027	0.0062	26.2	12.1	2.96	1.80	5.12	3.13	2.01	3.33	0.36	1.68
0.5	38.17	50.40	0.0029	0.0073	24.7	10.4	2.95	1.80	5.12	3.13	2.14	3.89	0.40	2.28
1	38.18	50.42	0.0031	0.0078	23.3	9.7	2.96	1.81	5.12	3.13	2.26	4.17	0.45	2.62
1.5	38.16	50.42	0.0029	0.0078	23.3	9.7	2.95	1.80	5.12	3.13	2.27	4.17	0.45	2.62
2	38.16	50.41	0.0027	0.0079	22.1	9.6	2.95	1.80	5.12	3.13	2.39	4.21	0.51	2.68

cantered cubic (FCC) structure. The prominent peaks at 38.16°, 44.18°, 64.23° and 77.21° of Bragg's reflections represent the (111), (200), (220), and (311) lattice planes of the FCC structure of silver, while the FCC structure of copper shows two sharp diffraction peaks appearing at 50.42° and 74.41° , which shares the lattice planes at (200) and (220). The increase in Ag concentration also increases the degree of crystallinity. The average crystallite sizes were calculated using Scherrer's equation

$$D = \frac{k\lambda}{\beta \cos \theta} \quad (1)$$

where $\lambda = 0.154$ nm is the wavelength of X-ray for CuKα, β is FWHM (full width at half maximum intensity of the peak), θ is the diffraction angle, and D is the crystallite size. Table 2 contains a summary of the values that were assigned to the crystallite size that was calculated. The concentration of silver has a direct relationship with the size of crystallites, while the concentration of copper has an inverse relationship with the size of crystallites. Due to the fact that the atomic radius of silver is greater than that of copper, the concentration of silver had an effect on the size of the crystallites that were present in the hybrid nanocomposite. The Williamson–Hall plot is shown in Fig. 1b and c, and in order to ascertain the strain as well as particle size, the intercept point on the Y-axis and the slope are calculated by fitting the given plot. The present investigation employed a Williamson–Hall analysis of silver nanocomposite under the assumption of uniform deformation, notwithstanding the model's failure to account for the fact that crystals exhibit spatial variation. Our system uniform displacement model for nanoparticles is depicted in Fig. 1

3.2 FT-IR study

Fig. 2 shows the Fourier-transform infrared spectra of the prepared nanocomposite. The bands that correspond to polyaniline are noticed at 1300, 1490, 1250, 1366, 1053, and 796 cm^{-1}. The conductivity peak at 1297 cm^{-1}, resulting from the C–N vibration of benzenoid rings, indicates that PANI is in its emeraldine salt form. As stated in ref. 30, the absorption peak at 802 cm^{-1} is caused by the aromatic ring. The absorption peaks at 795 cm^{-1} and 567 cm^{-1} are caused by the out-of-plane deformation of the C–H aromatic ring and the chloride group that forms a component of the PANI chain as well.[31] Further bands at 1003 cm^{-1} and 1047 cm^{-1} suggest the existence of resonance due

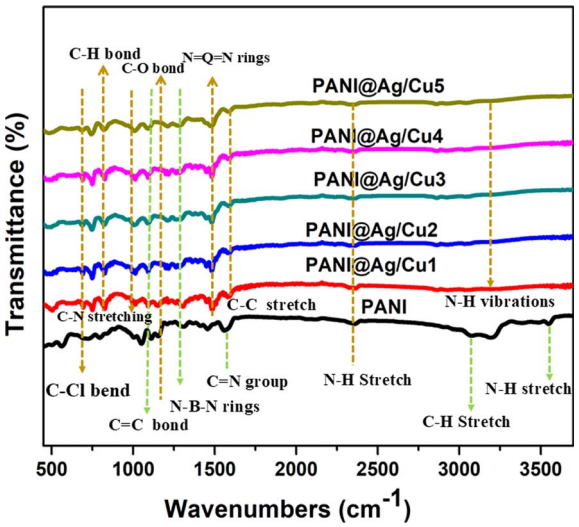

Fig. 2 The FTIR spectra of PANI and PANI@Ag/Cu hybrid nanocomposite with different concentration ratios of Ag/Cu.

to C–O stretching vibrations. A notable band at 1157 cm^{-1} generated by protonated chain vibration is observed in the nanocomposite, as shown in the figure. The N=Q=N and N–B–N stretching vibration bands are correspondingly observed at 1592 cm^{-1} and 1490 cm^{-1}. The polyaniline backbone benzenoid and quinoid groups are appropriately represented by –B– and =Q=. Also, the quinoid ring bands exhibit C–H and C=C stretching vibrations at 3074 cm^{-1} and 1458 cm^{-1}. The nanocomposite bands at 1146 cm^{-1} correspond to that of polyaniline. The absorption peaks at 1585 cm^{-1} and 1303 cm^{-1} are due to N–H bending vibrations of amino groups and C=C vibrations of benzenoid rings. The spectra of PANI and PANI@Ag/Cu hybrid nanocomposite displayed higher peak intensities. The peak of the N–H vibration was relocated from 3527 cm^{-1} to 3420 cm^{-1} due to the overlap between the two spectra. This shift is caused by a conjugated electron cloud composed of silver and copper nanoparticles as well as PANI chains.

3.3 Optical analysis and band gap values

Enhancing their potential applications requires research into the optical characteristics of PANI and PANI@Ag nanocomposite. Fig. 3 displays the ultraviolet-visible spectra of PANI.

Open Access Article. Published on 12 2024. Downloaded on 06.08.2025 02:01:24.
This article is licensed under a Creative Commons Attribution-NonCommercial 3.0 Unported Licence.

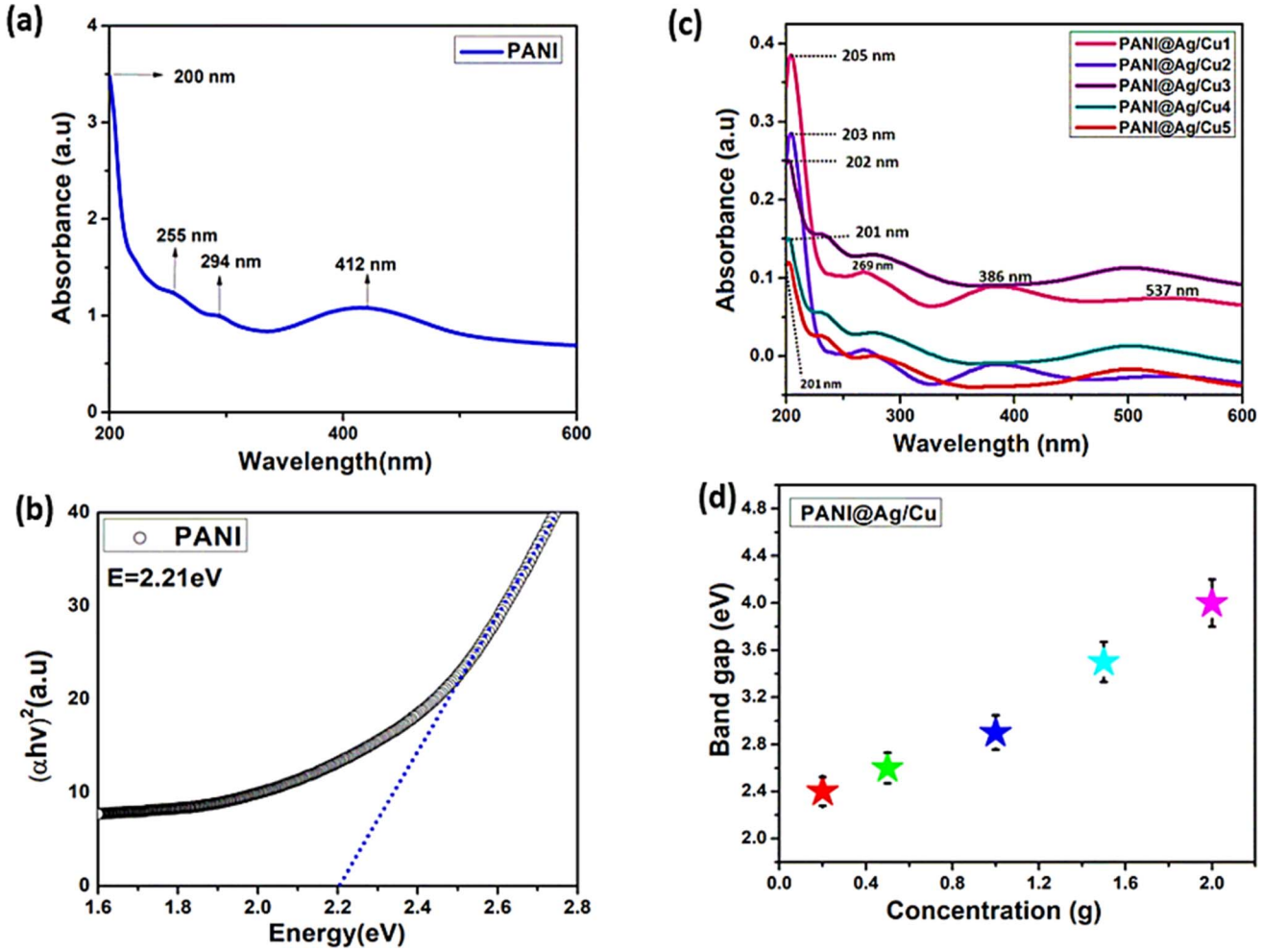

Fig. 3 (a) UV spectrum of (a) PANI (b) PANI@Ag/Cu hybrid nanocomposite (c) band gap of PANI and (d) band gap of PANI@Ag/Cu with various concentrations of the doped metal.

There are two absorption peaks at 255 nm and 412 nm, which represent the π–π* transition and the polaron band transitions. The samples of PANI@Ag/Cu hybrid nanocomposite were evaluated for the presence of silver and copper nanoparticles using UV-Vis absorption, as demonstrated in Fig. 3b. Fig. 3b shows that the spectra confirming the presence of silver and copper nanoparticles have the highest absorption bands at 205 nm, 203 nm, 202 nm, and 201 nm, respectively. In terms of absorption intensity, the PANI@Ag/Cu sample is outstanding. When the absorption peaks move to shorter wavelengths, it usually means the particle size or shape has changed, as a blue shift implies. When nanoparticles of silver and copper are doped into a PANI matrix, their surface plasmon resonance (SPR) characteristics can alter, leading to a shift in the absorption peaks. An essential metric for the hybrid nanocomposite electrical conductivity is the energy band gap.

$$\alpha = (h - E_g)^2/h\nu \quad (2)$$

As per Tauc's eqn (2), the direct allowed transition type can be used to approximatively determine the optical band gap of the powder sample.[32] Eqn (2) $\alpha = 2.303 \times 10^1\ A/Lc$ represents the absorption coefficient, where A is the sample absorbance, E_g is the optical band gap, h is the Planck constant, and ν is the reciprocal of the wavelength. L represents the path length, while A stands for absorption.[33] Based on the plot of $(\alpha h\nu)^2$ *vs.* $h\nu$, the E_g values of both the pure PANI and the produced hybrid nanocomposites have been calculated. In order to estimate the band gap, the straight line was extrapolated to the point where $(\alpha h\nu)^2 = 0$. As shown in Fig. 3c and d, the spectral analysis produced transition bandgaps (E_g) of around 2.21 eV for pure PANI, 2.4 eV for PANI@Ag/Cu_1, 2.6 eV for PANI@Ag/Cu_2, 2.9 eV for PANI@Ag/Cu_3, 3.5 eV for PANI@Ag/Cu_4, and 4.1 eV for PANI@Ag/Cu_5. Increases in the band gap allow the hybrid nanocomposite to potentially display optical features that can be varied, as shown in Fig. 3d. In a hybrid nanocomposite of PANI@Ag/Cu, the band gap is increased due to the specific interactions between the three materials. The incorporation of these metal nanoparticles into the PANI matrix causes alterations to the electrical structure of the polymer. Incorporating Ag and Cu nanoparticles into a nanocomposite can change its electrical characteristics by creating new energy levels in the band structure. The quantum confinement effect and changes in charge transfer dynamics

© 2024 The Author(s). Published by the Royal Society of Chemistry

Open Access Article. Published on 12 2024. Downloaded on 06.08.2025 02:01:24.
This article is licensed under a Creative Commons Attribution-NonCommercial 3.0 Unported Licence.

between the PANI and the metal nanoparticles can cause this modification to lead to an expanded band gap. These nanoparticles can also affect the PANI crystallinity and morphological properties, which in turn raises the band gap. The capacity to modify the emission and absorption spectra of the material by adjusting the band gap is a crucial characteristic of gas sensors. The energy levels at which electrons can be stimulated and then relax can be changed by changing the band gap of the sensor material. The material absorption and emission wavelengths may alter as a result of this change in energy levels. This allows for the possibility of tailoring the sensor to respond more strongly to certain gases by altering the energy levels at which they interact with the material. The ability to detect target gases at low concentrations with great precision is made possible by this characteristic, which enables the creation of highly selective gas sensors. It is possible to increase the adaptability and application of sensing technology by tuning the band gap, which in turn allows the development of sensors that work successfully for different types of gas molecules and in varied environmental situations.

3.4 Morphological analysis

Exhibited in Fig. 4a are the properties of pure PANI. Nanofibers, with diameters of around 100 nm and lengths of hundreds of nm to several micrometres, are clearly visible in this picture. Pure PANI is easily identifiable by the nanofibre agglomeration of inhomogeneous-shaped particles. Research conducted by Sheng Du *et al.* [34] suggests that aniline oligomers self-assemble to produce these nanofibers. Several factors, including π–π contact, hydrogen bonding, and van der Waals interactions, cause this self-assembly process. Although nanofibers are the most abundant component, the pure PANI structure does contain some aggregations. The morphology of prepared PANI@Ag/Cu hybrid nanocomposites was determined by FESEM images with low and high concentrations of doped metal in the PANI matrix, as shown in Fig. 4b and c. The image shows the silver and copper particles synthesized by the reduction of metal ions using hydrochloric acid, which resemble nano spherical with an average diameter of about 344 nm. In Fig. 4b, the images of PANI@Ag/Cu_1 clearly show non-agglomerated uniformly distributed silver and copper nanoparticles, as reported by Khanna *et al.*[35,36] In contrast, the illustration of aggregated silver and copper nanoparticles in a PANI matrix is shown in Fig. 4c. Particle interactions can be impacted by the structural changes detected in the host metal as a result of doping. Changes to the crystal structure that affect the agglomeration tendency may happen at higher concentrations of the PANI@Ag/Cu_5 hybrid nanocomposite. These spaces allow gas molecules to diffuse through the material, facilitating quick and efficient gas interaction with the sensor devices.

3.5 Dispersive X-ray spectroscopy (EDX)

Fig. 5 shows the EDS of PANI@Ag/Cu hybrid nanocomposite with different concentrations of Ag/Cu. The presence of carbon and nitrogen would be most prominently exhibited in an EDS analysis of pure polyaniline. These components make up the backbone of the polymer, as illustrated in Fig. 5a. Illustrations

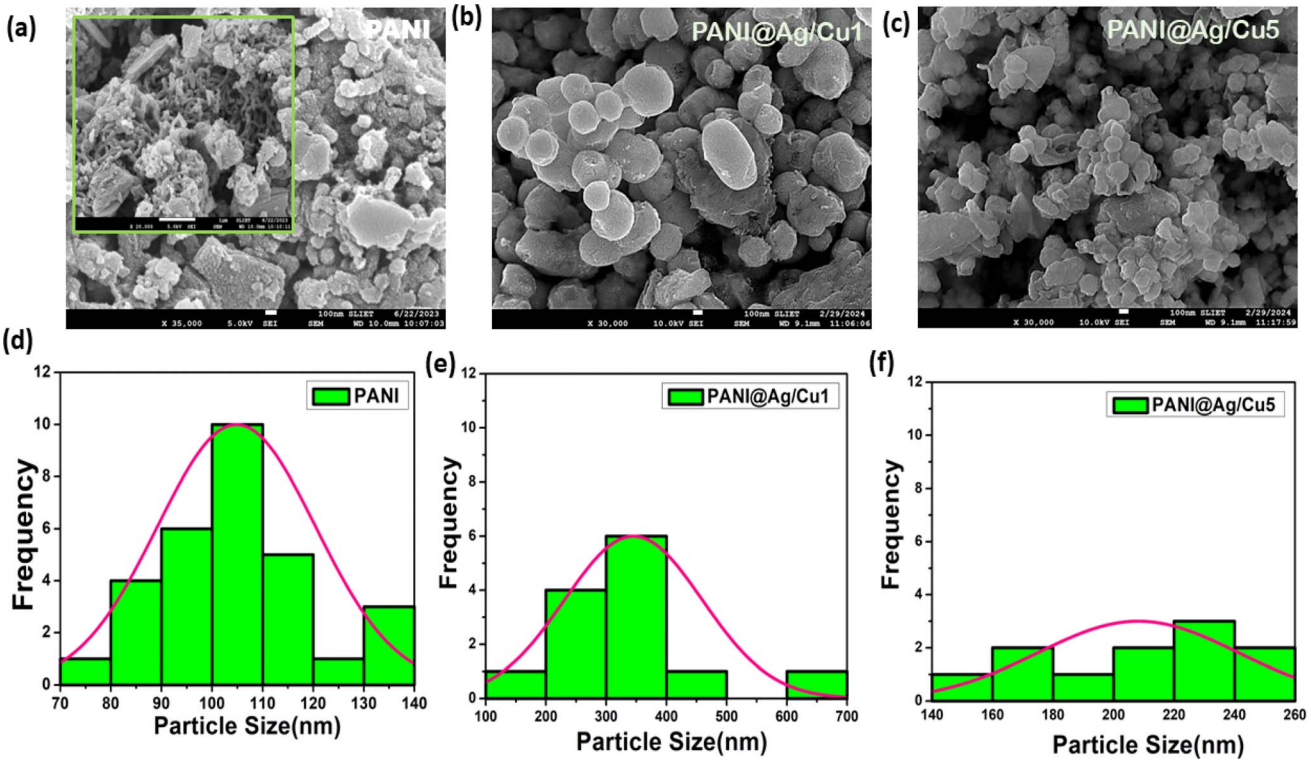

Fig. 4 FE-SEM of (a) PANI, (b and c) PANI@Ag/Cu hybrid nanocomposite with low and high concentrations and (d–f) particle size analysis of the sample.

Open Access Article. Published on 12 2024. Downloaded on 06.08.2025 02:01:24.
This article is licensed under a Creative Commons Attribution-NonCommercial 3.0 Unported Licence.

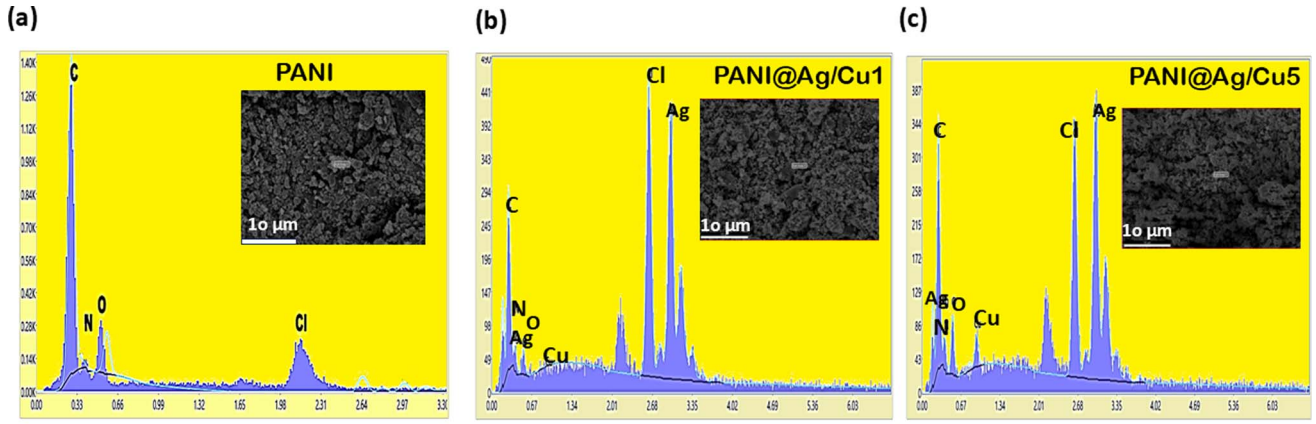

Element	Weight %	Atomic %
C	74.5	74.7
N	20.8	22.3
O	1.5	0.7
Cl	3.2	2.3

Element	Weight %	Atomic %
C	32.8	65.1
N	4.3	7.3
O	5.7	8.5
Cl	13.6	9.2
Cu	1.8	0.7
Ag	41.8	9.2

Element	Weight %	Atomic %
C	30.3	65.3
N	3.2	6.0
O	2.9	4.7
Cl	17.9	13.1
Cu	0.2	0.1
Ag	45.5	10.9

Fig. 5 EDX spectra of (a) PANI and (b and c) PANI@Ag/Cu hybrid nanocomposite.

indicate clearly that silver and copper nanoparticles can pass through the PANI matrix, as shown in Fig. 5b and c. Visual inspection confirmed the presence of Ag, Cu, N, and C in the PANI@Ag/Cu hybrid nanocomposite with low and high concentrations of doped nanoparticles. Since the H signal has a lower energy, it is not present. Moreover, the elements, namely Cl and O, came into being as a result of the addition of HCl and ammonium persulfate solution. Due to the fact that the surface is so important in gas detection, the properties of the fibre samples make them ideal for these uses.

3.6 Thermogravimetric (TG) and differential thermal analysis (DTA)

In order to comprehend further how ammonia adsorbs and desorbs from the sensor material, the weight fluctuations were examined using TG. A rise in mass following heating may suggest ammonia desorption, whereas a rise in mass upon cooling may indicate the opposite. Using a dynamic nitrogen flow and a heating rate of 100 °C min^{-1}, along with TGA and DTA experiments, the thermal stability of the synthesized PANI and typical PANI@Ag/Cu_1 hybrid nanocomposites was examined. The chemical shift of pure PANI caused by the TGA/DTA trace is shown in Fig. 6a. The sample lost 5.53% of its weight between ambient temperature and 100 °C when the adsorbed water molecules desorb. The kinetics of the reactions involved in ammonia sensing can be better understood by applying DTA to the thermal events. Improving sensor performance, including response and recovery times, can be achieved with the help of this data. The desorption was indicated by an endothermic peak at 156 °C on the DTA trace. The 100 to 203 °C range has no discernible impact on weight reduction. This demonstrates that the material has good heat resistance. Afterwards, the DTA trace revealed a large endothermic peak at 299.2 °C along with a consistent mass loss between 203 and 638 °C. Mass loss happens when the polymer burns, and this time, it was 42.46%. The nanocomposites undergo two stages of degradation: (a) the first weight loss was 2.01% and may be related to the loss of planar water; (b) the second weight loss was 5.15% due to degradation of polymeric chains and decomposition of polyaniline benzene ring-opening;[37] (c) the third weight loss was 27.2% at higher temperatures where complete combustion or decomposition of silver and copper in PANI matrix occurs. It is clear from these alterations that metallic nanoparticles have a significant impact on the thermal characteristics of nanocomposites. The results obtained from TGA confirmed that the PANI@Ag/Cu_1 hybrid nanocomposite is very stable under the temperature range of the thermal conductivity experiments in this work.

3.7 Gas sensing studies

3.7.1 The preparation of PANI film. A viscous solution was prepared by dissolving the emeraldine base form of PANI in *N*-methyl pyrrolidone (NMP). This solution was used to deposit the PANI layer on a silicon substrate using the spin coating method. The process was carried out at 1500 rpm for 20 seconds. Additionally, silver paste was used to create electrical connections on the polyaniline film.

3.7.2 The preparation of PANI@Ag/Cu nanocomposite film. In order to create a solution, the prepared PANI@Ag/Cu hybrid nanocomposite sample, which weighed 2 mg, was dissolved in polyvinyl pyrrolidone at a concentration of 0.1 M. The spin coating method was implemented in order to deposit a layer of PANI@Ag/Cu hybrid nanocomposite onto a silicon substrate, as depicted in Fig. 7. The procedure was carried out at

© 2024 The Author(s). Published by the Royal Society of Chemistry

Open Access Article. Published on 12 2024. Downloaded on 06.08.2025 02:01:24.
This article is licensed under a Creative Commons Attribution-NonCommercial 3.0 Unported Licence.

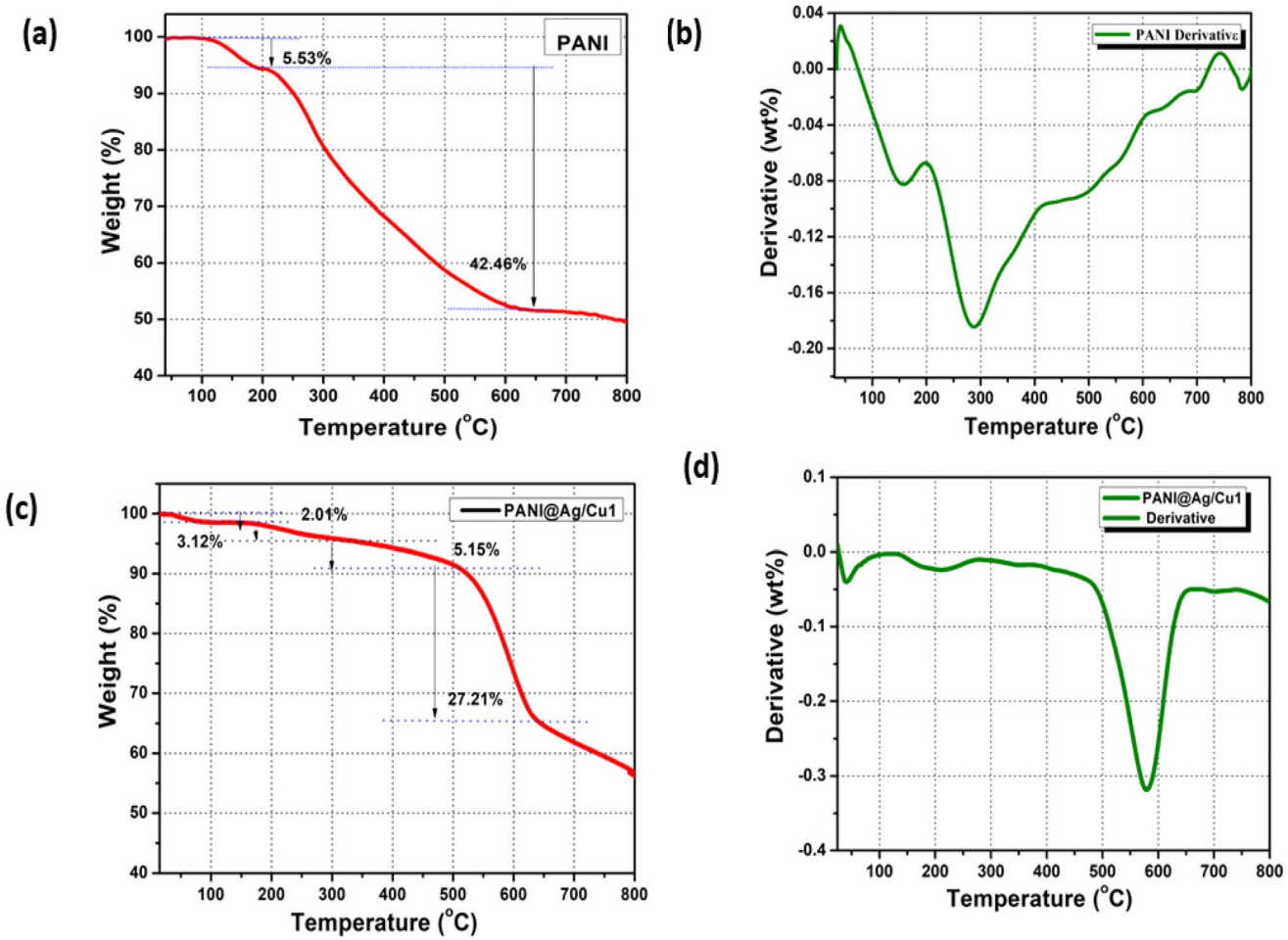

Fig. 6 (a and b) TG-DTA traces of pure PANI; (c and d) TG-DTA of PANI@Ag/Cu hybrid nanocomposite.

a speed of 1500 rpm for a duration of 10 seconds. Additionally, silver paste was used to create an electrical connection between the electrically created film.

3.7.3 Gas response of PANI@Ag/Cu hybrid nanocomposite film. Modulating the response/recovery cycle between varying NH_3 gas and metal-doped concentrations allows the sensor to respond to NH_3 gas. Fig. 8 shows the detection range of 100–300 ppm for NH_3 gas as a function of sensor resistance. There is little change in the resistance value of the pure PANI-based sensor when exposed to different concentrations of NH_3 gas. At the same time, as the concentration of NH_3 gas increases, the resistance values of sensors made of pure PANI and PANI@Ag/

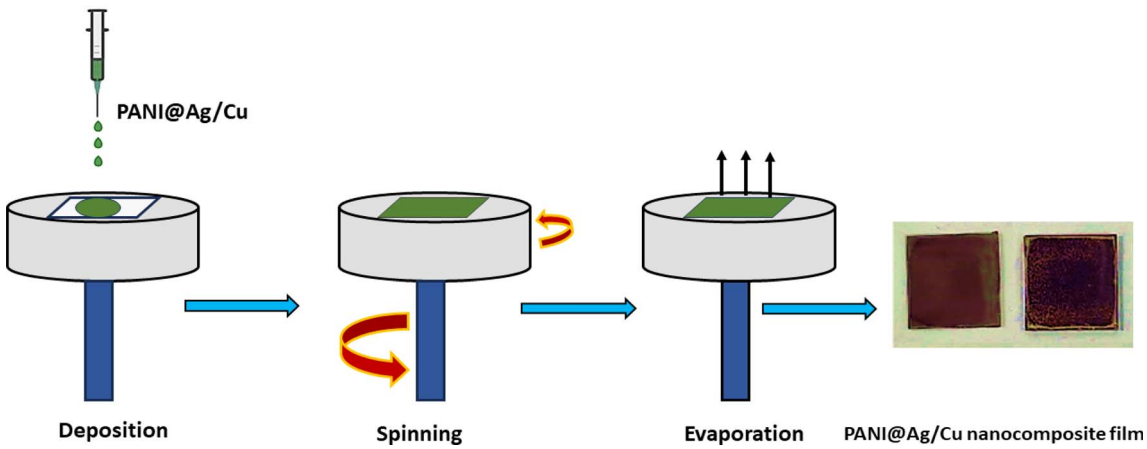

Fig. 7 PANI@Ag/Cu hybrid nanocomposite films for gas sensor using spin coating.

Open Access Article. Published on 12 2024. Downloaded on 06.08.2025 02:01:24.
This article is licensed under a Creative Commons Attribution-NonCommercial 3.0 Unported Licence.

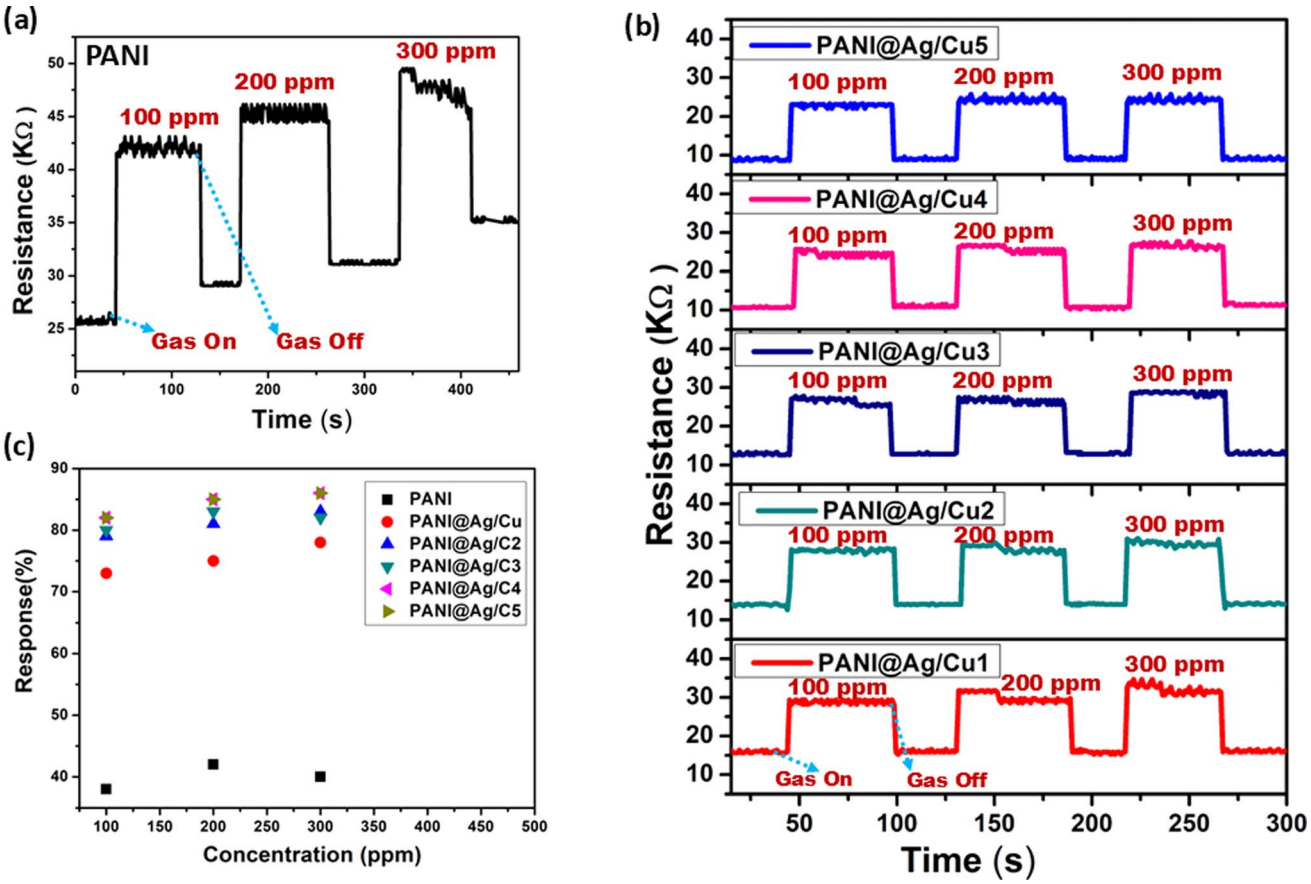

Fig. 8 (a) Transient resistance of gas sensors based on pure PANI; (b) the shift in resistance for different concentrations of Ag and Cu relative to time when exposed to NH_3 gas at room temperature (c) gas response of PANI and PANI@Ag/Cu with varying NH_3 concentrations.

Table 3 The response values of sensors prepared in this work regarding NH_3 gas

NH_3 gas concentration response (%)	100 ppm	200 ppm	300 ppm
PANI	38	42	40
PANI@Ag/Cu_1	73	75	78
PANI@Ag/Cu_2	79	81	83
PANI@Ag/Cu_3	80	83	82
PANI@Ag/Cu_4	82	85	86
PANI@Ag/Cu_5	82	85	86

Cu hybrid nanocomposite films with different concentrations of doped metal were observed to fall sharply, as shown in Fig. 8a and b. After each response/recovery time, when the test chamber is filled with air, the resistance values return to their approximate baseline levels. In particular, the resistance of the synthetic sensors for 100 ppm of ammonia gas varies from 15 kΩ to 29.3 kΩ for PANI@Cu/Ag_1 composites, 13.5 kΩ to 27.8 kΩ for PANI@Ag/Cu_2 composites, 12.7 kΩ to 26.8 kΩ for PANI@Ag/Cu_3 composites, 11.4 kΩ to 25.2 kΩ for PANI@Ag/Cu_4 composites, 8.7 kΩ to 23.1 kΩ for PANI@Ag/Cu_5 composites, and from 25.2 kΩ to 47.3 kΩ for the pure PANI film. Fig. 8c shows the hybrid nanocomposite conducting polymer sensor reactivity to ammonia gas. We created a bar graphic to show the gas sensor response to varying concentrations of ammonia. The bar chart clearly illustrates that the PANI sensor responds 38% to ammonia and 73% to PANI@Ag/Cu_5 at 100 ppm of NH_3 gas. This reveals that the PANI@Ag/Cu nanocomposite film sensor is suitable for real-time gas sensor design for NH_3 gas detection under atmospheric circumstances due to its excellent selectivity for this gas. Table 3 displays the response values of the sensors developed for this work with respect to the data in Fig. 8c shows these values against various concentrations of NH_3 gas.

3.7.4 Response and recovery time. Evaluating the response time and recovery duration of a sensor is important. The recovery time and response time of the sensor are critical for getting it back to its original state after gas removal. There are two ways to quantify them: first, the time it takes for the sensor to obtain 90% saturation of R_g from R_a during gas intake, and second, the value of R_a at 10% during gas withdrawal. In Fig. 9, the reaction and recovery period of pure PANI and PANI@Ag/Cu hybrid nanocomposite are displayed for various concentrations of NH_3 gas. Pure PANI response time jumps from 27 to 29 s and recovery time drops from 22 to 20 s as the NH_3 concentration goes up from 100 to 300 ppm. Reaction time drops to 12 s and recovery time jumps to 10 s for PANI@Ag/Cu_1, on the other hand. Due to the presence of Ag and copper ions in the PANI matrix, the PANI@Ag/Cu hybrid nanocomposite film has a quick recovery period. The PANI@Ag/Cu_3

© 2024 The Author(s). Published by the Royal Society of Chemistry

Open Access Article. Published on 12 2024. Downloaded on 06.08.2025 02:01:24.
This article is licensed under a Creative Commons Attribution-NonCommercial 3.0 Unported Licence.

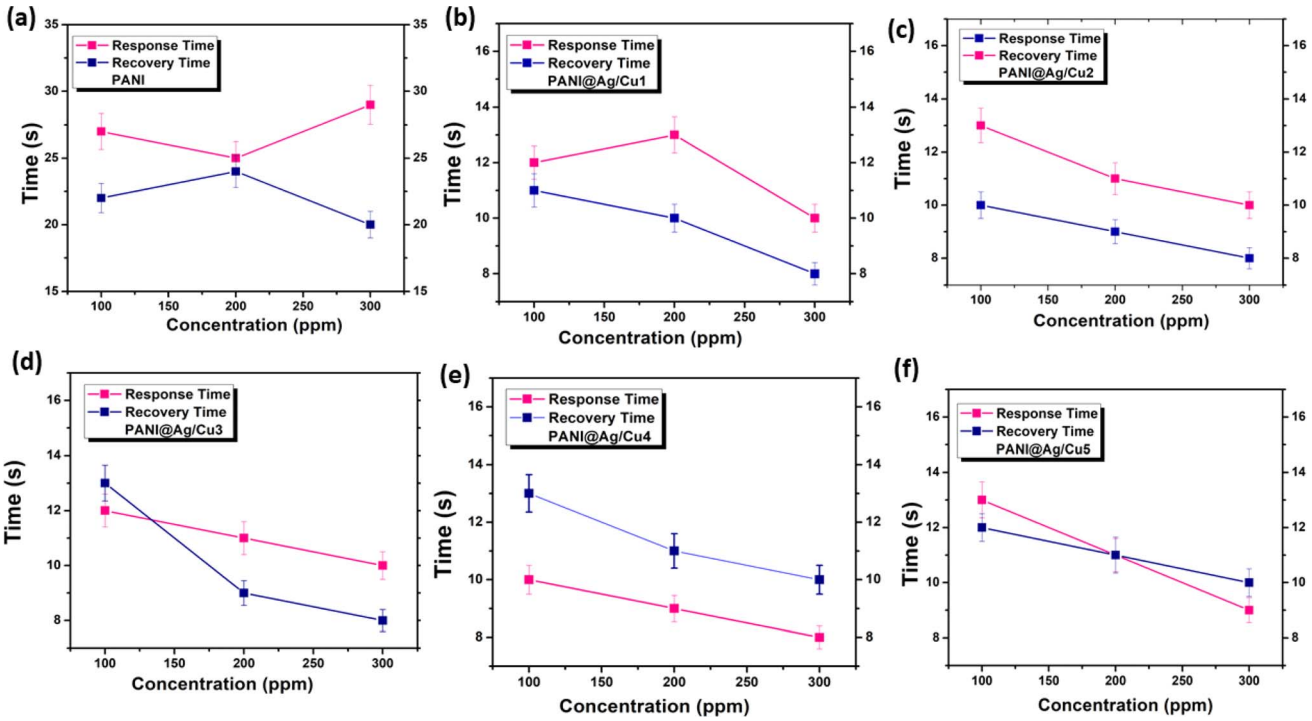

Fig. 9 . Response–recovery curves of gas sensors based on (a) pure PANI, (b) PANI@Ag/Cu_1 (c) PANI@Ag/Cu_2, (d) PANI@Ag/Cu_3, (e) PANI@Ag/Cu_4 and (f) PANI@Ag/Cu_5 hybrid nanocomposite when exposed to various concentrations of NH_3 gas at room temperature.

Table 4 Response times (T_1) and recovery times (T_2) of sensors under 100 ppm NH_3 gas

Sensitive films	Pure PANI	PANI@Ag/Cu_1	PANI@Ag/Cu_2	PANI@Ag/Cu_3	PANI@Ag/Cu_4	PANI@Ag/Cu_5
Response time (T_1)	27	12	10	12	10	13
Recovery time (T_2)	22	11	13	13	13	12

nanocomposite film has a minimum response time of around 8 s for 300 ppm. One possible explanation for the PANI@Ag/Cu sensor with high doping concentration showing impressive sensitivity to NH_3 gas is its rapid oxidation rate. Sensors made of PANI@Ag/Cu hybrid nanocomposites frequently have improved response and recovery time compared to sensors made of pure, as shown in Table 4 PANI. Fig. 9 and 10 show that the sensitivity, film response, and recovery time of

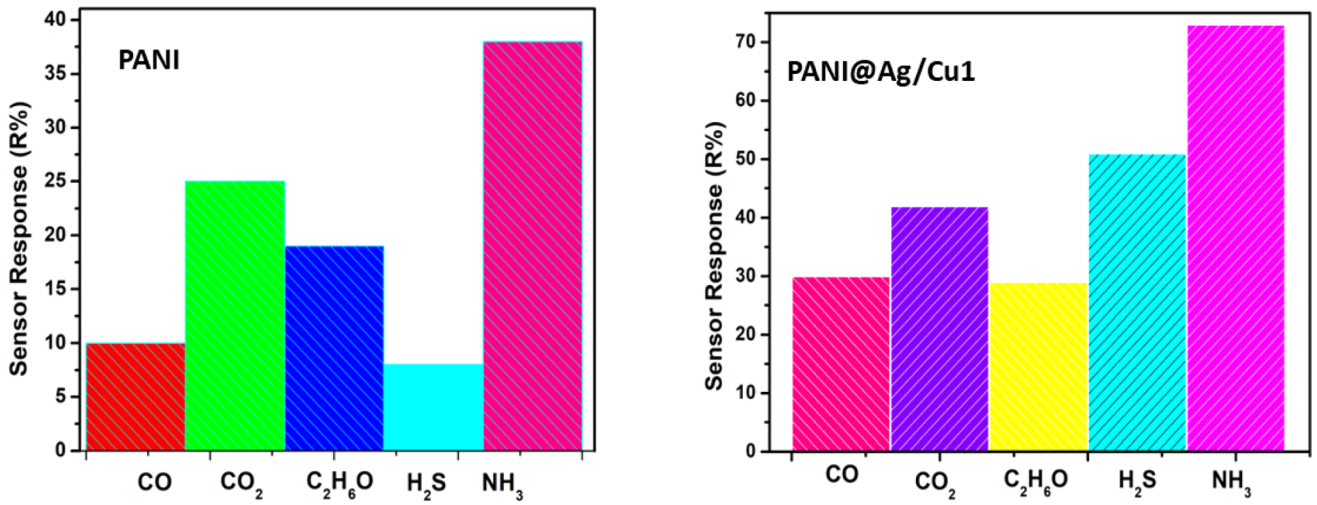

Fig. 10 Selectivity of PANI and PANI@Ag/Cu_1 hybrid nanocomposite gas sensors.

Open Access Article. Published on 12 2024. Downloaded on 06.08.2025 02:01:24.
This article is licensed under a Creative Commons Attribution-NonCommercial 3.0 Unported Licence.

Table 5 Comparison of PANI@Ag/Cu hybrid nanocomposite film-based ammonia sensor and those reported in the literature

Material	Multicomponent		Substrate	Temp.	Gas	ppm	Response (%)	T_1 (s)	T_2 (s)	Ref.
PAN1			PET	RT	NH_3	100	26	33	—	38
PANI			Si	RT	NH_3	50	1.65[b]	10	70	39
PANI			IDEs	RT	NH_3	290	6[b]	40	40	40
PANI				RT	NH_3	1000	20[b]	~2	~4	41
PANI			Glass	RT	NH_3	100	1.32[a]	300	560	42
PANI			Glass	RT	NH_3	10	22	—	—	43
PANI	ZnO	GO	IDE	RT	NH_3	50	38.31	<30		44
PANI	Au	TiO_2	Glass	RT	NH_3	10	48.6	52	122	45
PANI	Au	TiO_2	Glass	RT	NH_3	50	123	—	—	45
PANI	SnO_2	rGO	—	RT	NH_3	10	0.83	80		46
PANI	Au	In_2O_3	PET	RT		100	~46	118	144	47
PANI			Si	RT	NH_3	100–300	38–42	25–29	20–24	This work
PANI@Ag/Cu_1-5	Ag	Cu	Si	RT	NH_3	100–300	73–86	8–13	8–13	This work

[a] $A = (R_g - R_a)/R_a$. [b] $B = (I_a - I_g)/I_a$.

nanocomposites can be improved by varying the concentrations of silver and copper in the PANI matrix. It is possible that the good response and recovery times are caused by the *in situ* polymerization of PANI nanofibers onto silver and copper. This procedure creates a more even distribution of the nanofibers and increases their surface area, leading to improved room-temperature ammonia gas sensing performance. In Part 3.4, we discussed how to combine morphology and nanostructure investigations of PANI@Ag/Cu hybrid nanocomposites to find out how to increase the number of active sites for the adsorption of NH_3 gas molecules, which in turn reduces the recovery time and response time. Table 5 summarizes the research on NH_3 gas sensors and the PANI@Ag/Cu hybrid nanocomposite films compared to other sensors.

3.7.5 Selectivity. The selectivity of the PANI@Ag/Cu nanocomposite film sensors was examined in this study. At 100 ppm concentrations of NH_3 gas, ethanol (C_2H_5OH), carbon monoxide (CO), hydrogen sulphide (H_2S), and carbon dioxide (CO_2), the PANI@Cu_1 composites sensor responded as shown in Fig. 10. When compared to the other gases analysed, the PANI@Ag/Cu hybrid nanocomposite sensor clearly reacts much more strongly to NH_3 gas.

3.8 Sensing mechanism of PANI@Ag/Cu hybrid nanocomposite

A decrease in free charge carriers, which are partially consumed during complex formation as a result of the interaction between PANI and NH_3, an acceptor and a donor, respectively, causes the film resistance to increase with higher NH_3 intake. When the concentration of NH_3 gas increases, the system must shift in the direction dictated by Le Chatelier's primary equilibrium.[48] In contrast, the elimination of ammonia leads to a reversal of the system equilibrium. Ammonia gas has a greater electronegative charge due to nitrogen than hydrogen. With the addition of ammonia (NH_3) to PANI-based compounds, hydrogen atoms form a partial polar bond. An increase in the degree of inter-chain separation in PANI is the final result. There will be less opportunity for electron hopping, the fundamental conduction mechanism in PANI systems, between adjacent chains, leading to an increase in film resistance. The PANI emeraldine salt is transformed into the PANI emeraldine base form when the concentration of NH_3 vapor is greatest.[30] Following the removal of NH_3 vapour, the conversion of the emeraldine base back into emeraldine salt is all that is needed to restore the comprehensive performance of the sensor. Catalysing the reaction between PANI and ammonia can be achieved by including Ag/Cu nanoparticles in the composite. Potential benefits include increased sensitivity and quicker reaction times. Additionally, the ammonia molecules may be more easily adsorbed and dissociated by the metal nanoparticles. The local electromagnetic field can be amplified by silver nanoparticles due to their surface plasmon resonance (SPR), and with this improvement, the surface of the sensor may interact with ammonia molecules more effectively, which can boost its sensitivity. Silver makes electron transport processes faster, including sensing systems that use changes in electrical conductivity as their detection

© 2024 The Author(s). Published by the Royal Society of Chemistry

Open Access Article. Published on 12 2024. Downloaded on 06.08.2025 02:01:24.
This article is licensed under a Creative Commons Attribution-NonCommercial 3.0 Unported Licence.

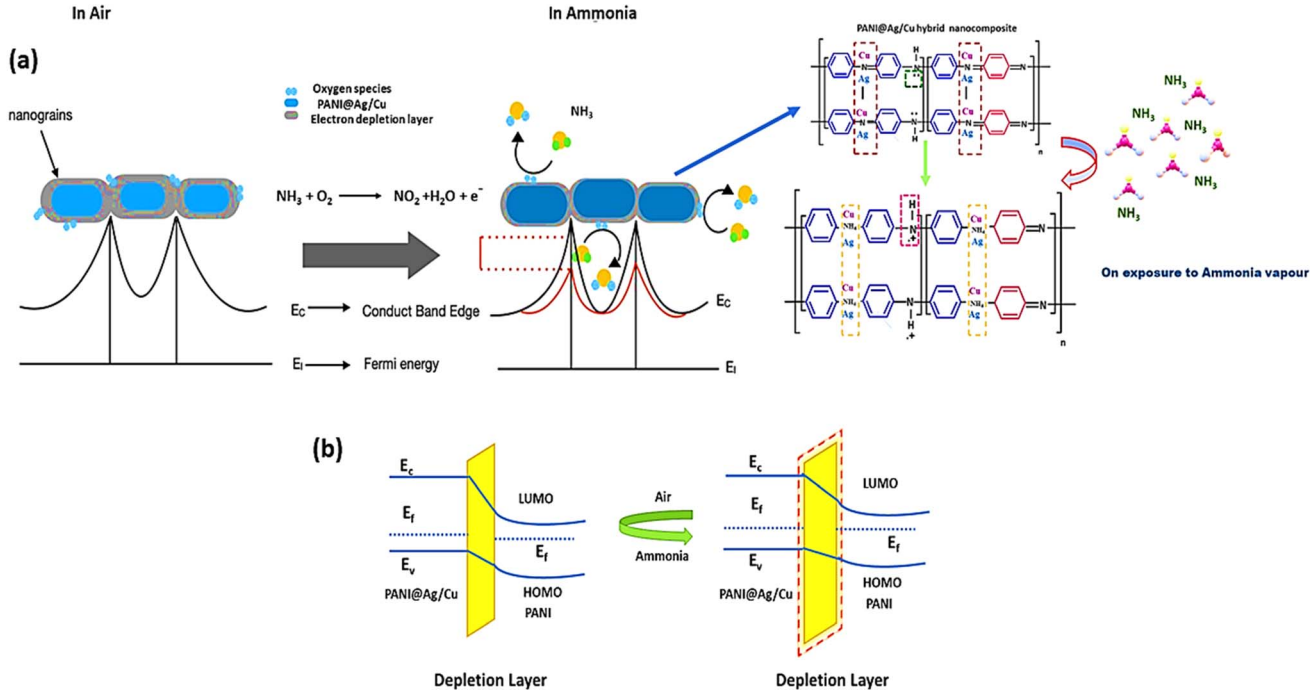

Fig. 11 (a) Schematic of ammonia sensing mechanism of sensors based on PANI@Ag/Cu hybrid nanocomposite; (b) energy band diagram of PANI@Ag/Cu hybrid nanocomposite during the gas sensing reaction process.

method. The rapid reaction to ammonia is due to the excellent electron transport routes that Ag can provide. In addition, copper is highly conductive electrically and crucial for detecting the changes in electrical characteristics upon ammonia exposure, and when added to the nanocomposite, it can improve the overall conductivity of the sensor. A higher surface area for the nanocomposite is possible with the addition of silver/copper nanoparticles. Since there are more active sites for ammonia adsorption on a bigger surface area, the sensor is more sensitive and responsive. A synergistic effect is generated when PANI is combined with silver and copper, greatly increasing the sensor sensitivity. When combined, distinct characteristics of Ag/Cu, including high conductivity, catalytic activity, and SPR, improve the sensing performance as a whole. Having both metals in the sensor can make it more sensitive to ammonia and less sensitive to other gases. Ammonia can be more efficiently adsorbed and detected when using a combination of metals since each metal may have a unique interaction with different gases. Ag and Cu on the PANI matrix can make it more chemically and thermally stable. A longer-lasting sensor that performs well in a wide range of environments is the result of this improvement. Nevertheless, the PANI@Ag/Cu hybrid nanocomposite surface uses chemical interaction with ammonia molecules for detection. Various interactions between the ammonia molecules and the silver/copper nanoparticles can occur, including hydrogen bonds, dipole–dipole interactions, or weak chemical bonds. These interactions have the potential to alter the electrical properties of the composite material, such as its conductivity and other quantifiable aspects. The NH_3 detection technique of PANI and PANI@Ag/Cu nanocomposite films is illustrated schematically in Fig. 11.

4. Conclusion

In conclusion, PANI@Ag/Cu hybrid nanocomposite thin films were synthesized by chemical oxidative polymerization of aniline monomer to be applied as gas sensors. Ag/Cu concentrations were varied to find the optimum concentration to detect ammonia. XRD analysis indicates the formation of the crystalline Ag and Cu nanoparticles on (111) lattice planes. The crystallite sizes decrease with increasing Ag and Cu concentrations. FTIR spectra show the bonding of N–H in the polyaniline structure. UV-vis absorption spectra confirmed the formation of Ag and Cu nanoparticles in the PANI matrix and the resonance plasmon band located at around 201 to 205 nm. The result shows that the PANI@Ag/Cu_3 nanocomposite thin film displayed a good response of approximately 86%, with response and recovery periods of 10 and 8 s among the other synthesized samples. It indicates that the increment of Ag and Cu concentrations enhanced ammonia gas sensing performance at room temperature. The PANI@Ag/Cu hybrid nanocomposite exhibits excellent gas-sensing properties for ammonia due to the combined effects of conductivity change, protonation and interactions with the metal nanoparticles. This makes these nanocomposites effective for use in gas sensors, providing high sensitivity and selectivity for detecting ammonia gas. In this study, we have tested the sensors over a limited range of gas concentrations. Real-world applications might involve a broader and more variable range of concentrations. The sensor selectivity towards specific gases in the presence of other interfering gases has not been thoroughly evaluated. The long-term stability and durability of the PANI nanocomposite sensors need to be tested.

Open Access Article. Published on 12 2024. Downloaded on 06.08.2025 02:01:24.
This article is licensed under a Creative Commons Attribution-NonCommercial 3.0 Unported Licence.

Data availability

The data used to support the findings of this study are available from the corresponding author upon request.

Conflicts of interest

The authors declared no conflict of interest.

References

1 C. Nylabder, M. Armgrath and I. Lundstrom, An ammonia detector based on a conducting polymer, *Proceedings of the International Meeting on Chemical Sensors*, Fukuoka, Japan, 1983, pp. 203–207.
2 A. Verma, G. Rajeev, S. V. Ajay and T. Kumar, A review of composite conducting polymer-based sensors for detection of industrial waste gases, *Sens. Actuators Rep.*, 2023, **5**, 100143.
3 A. Huda, N. M. Naim, N. A. N. Azmy and A. A. Hamid, PANI-Ag-Cu Nanocomposite Thin Films Based Impedimetric Microbial Sensor for Detection of E. coli Bacteria, *J. Nanomater.*, 2014, **1**, 951640.
4 S. M. Reda and S. M. Al-Ghannam, Synthesis and electrical properties of polyaniline composite with silver nanoparticles, *Adv. Mater. Phys. Chem.*, 2012, **2**, 75–81.
5 G. B. V. S. Lakshmi, M. Alam, A. M. Siddiqui, M. Zulfequar and M. Husain, Synthesis and characterization of Se doped polyaniline, *Curr. Appl. Phys.*, 2011, **11**(2), 217–222.
6 S. C. K. Misra, P. Mathur, M. Yadav, M. K. Tiwari, S. C. Garg and P. Tripathi, Preparation and characterization of vacuum deposited semiconducting nanocrystalline polymeric thin film sensors for detection of HCl, *Polymer*, 2004, **45**(25), 8623–8628.
7 S. C. K. Misra, P. Mathur and B. K. Srivastava, Vacuum-deposited nanocrystalline polyaniline thin film sensors for detection of carbon monoxide, *Sens. Actuators, A*, 2004, **114**(1), 30–35.
8 B. Lai, P. Wang, H. Li, Z. Du, L. Wang and S. Bi, Calcined polyaniline- iron composite as a high efficient cathodic catalyst in microbial fuel cells, *Bioresour. Technol.*, 2013, **131**, 321–324.
9 Z. Mo, H. Peng, H. Liang and S. Liao, Vesicular nitrogendoped carbon material derived from Fe_2O_3 templated polyaniline as improved non-platinum fuel cell cathode catalyst, *Electrochim. Acta*, 2013, **99**, 30–37.
10 K.-J. Huang, J.-Z. Zhang, Y.-J. Liu and L.-L. Wang, Novel electrochemical sensing platformbased on molybdenum disulfide nanosheets-polyaniline composites and Au nanoparticles, *Sens. Actuators, B*, 2014, **194**, 303–310.
11 H. Xu, J. Li, Z. Peng, J. Zhuang and J. Zhang, Investigation of polyaniline films doped with Ni2+ as the electrode material for electrochemical supercapacitors, *Electrochim. Acta*, 2013, **90**, 393–399.
12 G. Yang, M. Zhang, D. Dong, *et al.*, TiO2 based sensor with butterfly wing configurations for fast acetone detection at room temperature, *J. Mater. Chem. C*, 2019, **7**, 11118–11125.
13 L. He, Y. Liu, J. Liu, *et al.*, Core-shell noble-metal@metalorganic-framework nanoparticles with highly selective sensing property, *Angew. Chem., Int. Ed.*, 2013, **52**, 3741–3745.
14 A. A. Athawale, S. V. Bhagwat and P. P. Katre, Nanocomposite of Pd–polyaniline as a selective methanol sensor, *Sensor. Actuator. B Chem.*, 2006, **114**, 263–267.
15 S. Jiang, J. Chen, J. Tang, *et al.*, Au nano particles-functionalized two-dimensional patterned conducting PANI nanobowl monolayer for gas sensor, *Sensor. Actuator. B Chem.*, 2009, **140**, 520–524.
16 A. Choudhury, Polyaniline/silver nanocomposites: dielectric properties and ethanol vapour sensitivity, *Sensor. Actuator. B Chem.*, 2009, **138**, 318–325.
17 U. V. Patil, N. S. Ramgir, N. Karmakar, *et al.*, Room temperature ammonia sensor based on copper nanoparticle intercalated polyaniline nanocomposite thin films, *Appl. Surf. Sci.*, 2015, **339**, 69–74.
18 L. Hong, Y. Li and M. Yang, Fabrication and ammonia gas sensing of palladium/polypyrrole nanocomposite, *Sensor. Actuator. B Chem.*, 2010, **145**, 25–31.
19 C. V. Tuan, M. A. Tuan, N. V. Hieu, *et al.*, Electrochemical synthesis of polyaniline nanowires on Pt interdigitated microelectrode for room temperature NH3 gas sensor application, *Curr. Appl. Phys.*, 2012, **12**, 1011–1016.
20 G. Shivam Kumar and P. Siddhartha, Highly sensitive Cu-ethylenediamine/PANI composite sensor for NH3 detection at room temperature, *Talanta*, 2023, **258**, 124418.
21 J. Zhang, P. Guan, W. Li, Z. Shi and H. Zhai, Synthesis and characterization of a polyaniline/silver nanocomposite for the determination of formaldehyde, *Instrum. Sci. Technol.*, 2016, **44**(3), 249–258.
22 S. Cuiab, J. Wang and X. Wang, Fabrication and design of a toxic gas sensor based on polyaniline/titanium dioxide nanocomposite film by layer-by-layer self-assembly, *RSC Adv.*, 2015, **5**, 58211–58219.
23 S. J. Park, O. S. Kwon and J. Jang, A high-performance hydrogen gas sensor using ultrathin polypyrrole-coated CNT nanohybrids, *Chem. Commun.*, 2013, **49**, 4673–4675.
24 Y. Yin, H. Zhang, P. Huang, *et al.*, Inducement of nanoscale Cu–BTC on nanocomposite of PPy–rGO and its performance in ammonia sensing, *Mater. Res. Bull.*, 2018, **99**, 152–160.
25 D. Zhang, Z. Wu and X. Zong, Metal-organic frameworks-derived zinc oxide nanopolyhedra/S, N: graphene quantum dots/polyaniline ternary nanohy_brid for high-performance acetone sensing, *Sensor. Actuator. B Chem.*, 2019, **288**, 232–242.
26 R. K. G. Bavane, A. M. Mahajan, M. D. Shirsat and R. B. Gore, Ammonia Gas Sensing Characteristics of Spin Coated Polyaniline Films, *Adv. Phys.*, 2013, **3**(3), 241–248.
27 J. A. Hassan, *et al.*, Sensing Characteristics of Nanostructured PANI/Ag Thin Films as H_2 S Gas Sensor, *Mater. Sci. Eng.*, 2020, **928**, 072146.
28 M. L. Mota, A. Carrillo, A. J. Verdugo, A. Olivas, J. M. Guerrero, E. C. De la Cruz and N. Noriega Ramírez, Synthesis and Novel Purification Process of PANI and PANI/AgNPs Composite, *Molecules*, 2019, **24**(8), 1621.

© 2024 The Author(s). Published by the Royal Society of Chemistry

Open Access Article. Published on 12 2024. Downloaded on 06.08.2025 02:01:24.
This article is licensed under a Creative Commons Attribution-NonCommercial 3.0 Unported Licence.

29 A. D. Bhagwat, S. S. Sawant and C. M. Mahajan, Facile rapid synthesis of polyaniline (PANI) nanofibers, *J. Nano- Electron. Phys.*, 2016, **8**(1), 8–10.
30 Z. Pang, Z. Yang, Y. Chen, J. Zhang, Q. Wang, F. Huang and Q. Wei, *Colloids Surf., A*, 2016, **494**, 248–255.
31 G. Otrokhov, D. Pankratov, G. Shumakovich, M. Khlupova, Y. Zeifman, I. Vasil'eva and A. Yaropolov, Enzymatic oligomerization and polymerization of arylamines: state of the art and perspectives, *Electrochim. Acta*, 2014, **123**, 151–157.
32 S. Dhibar and C. K. Das, Transition metal-doped polyaniline/single-walled carbon nanotubes nanocomposites: Efficient electrode material for high performance supercapacitors, *Ind. Eng. Chem. Res.*, 2014, **53**, 3495–3508.
33 P. Chrysicopoulou, D. Davazoglou, C. Trapalis and G. Kordas, Optical properties of very thin (< 100 nm) sol–gel TiO2 films, *Thin Solid Films*, 1998, **323**, 188.
34 X.-S. Du, C.-F. Zhou, G.-T. Wang and Y.-W. Mai, Since 2023 Since 2022 Since 2019 Custom range… Sort by relevance Sort by date Any type Review articles Novel solid-state and template-free synthesis of branched polyaniline nanofibers, *Chem. Mater.*, 2008, **20**, 3806–3808.
35 P. K. Khanna, S. Gaikwad, P. V. Adhyapak, N. Singh and R. Marimuthu, Synthesis and characterization of copper nanoparticles, *Mater. Lett.*, 2007, **61**(25), 4711–4714.
36 P. K. Khanna, N. Singh, S. Charan, V. V. V. S. Subbarao, R. Gokhale and U. P. Mulik, Synthesis andcharacterizationofAg/PVA nanocomposite by chemical reduction method, *Mater. Chem. Phys.*, 2005, **93**(1), 117–121.
37 V. Tauc and A. Menth, States in the gap, *J. Non-Cryst. Solids*, 1972, **8–10**, 569–585.
38 D. K. Bandgar, S. T. Navale, S. R. Nalage, R. S. Mane, F. J. Stadler, D. K. Aswal, S. K. Gupta and V. B. Patil, Simple and low-temperature polyaniline-based flexible ammonia sensor: A step towards laboratory synthesis to economical device design, *J. Mater. Chem.*, 2015, **3**, 9461–9468.
39 A. L. Sharma, K. Kumar and A. Deep, *Sensor Actuator Phys.*, 2013, **198**, 107.
40 P. Lobotka, P. Kunzo, E. Kovacova, I. Vavra, Z. Krizanova, V. Smatko, J. Stejskal, E. N. Konyushenko, M. Omastova, Z. Spitalsky, M. Micusik and I. Krupa, *Thin Solid Films*, 2011, **519**(12), 4123.
41 S. Z. Wu, F. Zeng, F. X. Li and Y. L. Zhu, *Eur. Polym. J.*, 2000, **36**(4), 679.
42 C. J. Liu, Z. Noda, K. Sasaki and K. Hayashi, *Int. J. Hydrogen Energy*, 2012, **37**(18), 13529.
43 Q. X. Nie, Z. Y. Pang, D. W. Li, H. M. Zhou, F. L. Huang, Y. B. Cai, *et al.*). Facile fabrication of flexible SiO2/PANI nanofibers for ammonia gas sensing at room temperature, *Colloids Surf., A*, 2018, **537**, 523–539, DOI: **10.1016/j.colsurfa.2017.10.065**.
44 R. S. Andre, F. M. Shimizu, C. M. Miyazaki, *et al.*, Hybrid layer-by-layer (LbL) films of polyaniline, graphene oxide and zinc oxide to detect ammonia, *Sensor. Actuator. B Chem.*, 2017, **238**, 795–801.
45 B. Li and D. N. Lambeth, *Nano Lett.*, 2008, **8**(11), 3563.
46 H. H. Lu, C. Y. Lin, T. C. Hsiao, Y. Y. Fang, K. C. Ho, D. Yang, C. K. Lee, S. M. Hsu and C. W. Lin, *Anal. Chim. Acta*, 2009, **640**(1–2), 68.
47 S. Sharma, S. Hussain, S. Singh, *et al.*, MWCNTconducting polymer composite based ammonia gas sensors: A new approach for complete recovery process, *Sensor. Actuator. B Chem.*, 2014, **194**, 213–219.
48 K. Crowley, A. Morrin, A. Hernandez, E. O'Malley, P. G. Whitten, G. G. Wallace, M. R. Smyth and A. J. Killard, *Talanta*, 2008, **77**, 710–717.